The Korean Journal of Ceramics, 7[1] 6-10 (2001)

Electrical Properties of Ultrafine $(CeO_2)_{0.9}(Gd_2O_3)_{0.1}$ Powders Prepared by Glycine Nitrate Process for the High Efficient Solid Oxide Fuel Cell Applications

Kang-Ryeol Lee and Sung Park†

Departement of Ceramic Engineering, Myong Ji University, Kyunggi-do, 449-728, Korea

(Receoved March 7, 2000 · Accepted November 27, 2000)

Ultrafine $(CeO_2)_{0.9}(Gd_2O_3)_{0.1}$ solid solution powders synthesized by the glycine-nitrate process, with specific surface areas of 19~23 m^2/g were sintered at 1500°C for various sintering times and then their electrical characteristics were investigated using AC impedance and four-point probe measurements. The electrical resistivity of the sintered $(CeO_2)_{0.9}(Gd_2O_3)_{0.1}$ bodies showed the minimum value at the sintering time of 10 hrs. The minimum total resistivity of the $(CeO_2)_{0.9}(Gd_2O_3)_{0.1}$ bodies sintered at 1500°C for 10 hrs seems to result from the lowest activation energy for the electrical resistivity by the combination between the activation energies for the resistivities at the grain interior and grain boundary.

Key words: Electrical Properties, Ultrafine Powders, $(CeO_2)_{0.9}(Gd_2O_3)_{0.1}$, Glycine-Nitrate Process, Solid Oxide Fuel Cells

I. Introduction

The state-of-the art solid oxide fuel cells (SOFCs) operate at 1000°C. It is generally desirable to reduce the operating temperature of SOFC to make them competitive with other types of fuel cells and to avoid the high temperature interaction and interdiffusion that take place between cell components. This can be easily achieved by developing the technology for new electrolytes that operate efficiently with reduced interaction and lower resistivity at lower temperatures.[1] The doped CeO_2, candidate as a new electrolyte material for the development of intermediate temperature SOFC, has the maximum electrical conductivity at the amount of dopants which yields approximately 5% of the oxygen sublattice site vacant in the CeO_2 solid solution.[1-5] This corresponds to either dopant additions of 10 mol% of a bivalent cation or 20 mol% of a trivalent cation.

On the other hand, a few studies have been conducted to prepare the fine CeO_2 powders using the methods such as hydro-thermal synthesis and homogeneous precipitation.[6, 7] Recently, the glycine-nitrate process (GNP) has been introduced as an one of a general class of combustion methods for the preparation of ceramic powders.[8] A highly viscous mass formed by evaporation of a solution of metal nitrates as an oxidizer and glycine as a fuel is ignited to produce the ultrafine ceramic powders in this process. The very fine size and crystalline nature of the powder by the GNP are believed to be direct result of the short exposure to high temperatures during the ignition step. The GNP also offers a relatively inexpensive route to the preparation of very fine and chemically homogeneous powders. It has been used for the preparation of simple oxides as well as multicomponent oxides.[9, 10]

Therefore, there is an ample interest for synthesizing the ultrafine Gd-doped CeO_2 powders with high electrical conductivity by the GNP. In this paper, we present the results of investigations of electrical properties of sintered $(CeO_2)_{0.9}(Gd_2O_3)_{0.1}$ bodies produced using the ultrafine powders synthesized by the GNP.

II. Experimental Procedure

The raw materials such as $Ce(NO_3)_{36}H_2O$ (Aldrich, USA, purity 4N), $Gd(NO_3)_{26}H_2O$ (Aldrich, USA, purity 5N), and glycine (NH_2-CH_2-COOH) (Junsei, Japan) were used as oxidizer and fuel for GNP, respectively. The Gd_2O_3 content in the Gd-doped CeO_2 powder was adjusted to be 10 mol% to yield 5% of the oxygen sublattice site vacant by calculating the cation amounts of metal salts. After these metal salts and fuel were dissolved in an appropriate distilled water, this solution was stirred and heated on a hot plate to evaporate the distilled water, and then finally self-ignited in a domestic microwave oven with the output power of 750W. When the distilled water becomes fully vaporized, spontaneous combustion starts by burning of metal salts and glycine. As a result, the Gd-doped CeO_2 powders were formed with

†Corresponding author: spark@wh.myongji.ac.kr

gases of N_2, CO_2 and H_2O releasing. Here, the amounts of glycine and metal salts were controlled by accounting for the balance of oxidizing. Valences and reducing valences among the reactants according to Jain.[11] The reaction products were calcined for 2 hrs at 650°C to remove any carbon residues remaining on the synthesized oxide powder obtained. The synthesized powders after calcination were milled in ethyl alcohol using ZrO_2 ball and the 3-dimensional mixer of 60 cycle/min for 4 hrs. The green bodies for sintering were made by uniaxial pressing with the pressure of 50 kg_f/cm^2 and then sintered at 1500°C with various sintering times in air. The heating rate for sintered bodies was maintained to be constant of 4°C/min. The electrical properties of the sintered bodies were measured mainly by an AC two-terminal method and specially at 800°C by a four-probe method. For the measurements the sintered bodies were made with the button type (7 mm diameter 1.5mm thickness). Platinum electrodes were made from paste and attached to both surfaces and then backed at 1050°C for 0.5 hr. Electrical contact was made by clamping the sample between platinum foil in high purity Al_2O_3 disks. Resistivity was measured at temperature from 200°C to 800°C in air, using an impedance analyzer (Hp 4192A LF, Hewlett-Packard, CA) at a frequency range of 5 Hz to 13 MHz. Temperature for the measurement were controlled within ±1.

III. Results and Discussion

The uniaxially pressed $(CeO_2)_{0.9}(Gd_2O_3)_{0.1}$ green bodies were sintered at 1500°C for various sintering time in air and then electrical resistivity of sintered bodies was measured with AC impedance method in air. The grain interior and grain boundary resistivities to make up the total resistivity of the specimens were measured from the sizes of arcs for complex impedance plot as shown in fig. 1. Fig. 1 shows typical complex impedance plots for the pure CeO_2 and $(CeO_2)_{0.9}(Gd_2O_3)_{0.1}$ bodies which were sintered at 1500°C for 10 hrs and then measured at 325°C and 250°C in air, respectively, where the R axis is real and the Z axis is imaginary. It is possible to identify the grain interior and grain boundary resistivities from the visible arcs on the impedance plots obtained from the impedance spectroscopy measurements.[12] These arcs are due to be caused by polarization within the grain interior and grain boundary from left to right. From the typical impedance plots, it can be seen that the sintered $(CeO_2)_{0.9}(Gd_2O_3)_{0.1}$ body has much lower total resistivity in comparison with that of the sintered pure CeO_2 body, which consists of low grain interior resistivity and high grain boundary resistivity at the measured temperature. It can be, therefore, said that the total resistivity of the sintered pure CeO_2 body was reduced by the formation of oxygen vacancies, which Gd_2O_3 doping has induced, and the total resistivity of the sintered $(CeO_2)_{0.9}(Gd_2O_3)_{0.1}$ body is mainly ascribed to the grain boundary resistivity unlikely that of the sintered CeO_2 body.

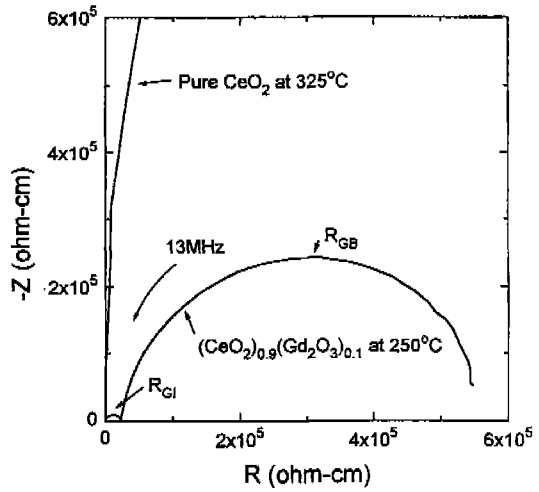

Fig. 1. Typical complex impedance plot for the sintered CeO_2 and $(CeO_2)_{0.9}(Gd_2O_3)_{0.1}$ bodies at 1500°C, where RGI and RGB indicate the grain interior(GI) and grain boundary(GB) resistivities from the two arcs visible in the complex impedance plots, respectively.

Fig. 2 shows the impedance spectra for the sintered $(CeO_2)_{0.9}(Gd_2O_3)_{0.1}$ bodies that were sintered at 1500°C for

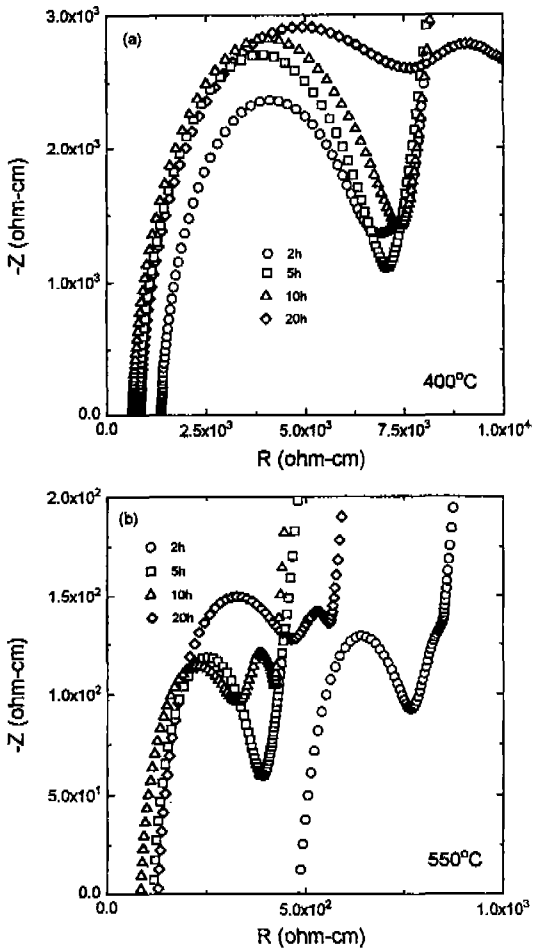

Fig. 2. Complex impedance spectra for the specimens that were sintered at 1500°C for various time and then were measured at 400°C (a) and 550°C (b) in air.

the various times and then were measured at 400°C (Fig. 2(a)) and 550°C (Fig. 2(b)) in air. The arc corresponding to grain interior resistivity is not shown in the impedance spectra at these measuring temperatures due to rapid movement of ionic species or vacancies by high measuring temperatures. The third arcs corresponding to the interfacial polariza-tion[13] between the specimen and the platinum electrode are additionally displayed in these figures. As the measuring temperature increases the sized of arcs corresponding to grain boundary resistivity shrink greatly, showing the smallest arc for the specimen at the sintering time of 10 hrs in Fig. 2(b). It means that the electrical resistivity of specimen decreases with the increase or the measuring temperature and that of the specimen at the sintering time of 10hrs has the smallest value at 550°C.

On the other hand, the specimen sintered for 20 hrs has the largest grain boundary resistivity with the largest size of the arc corresponding to the grain boundary resistivity regardless of the measuring temperatures. Despite that the specimen sintered at 1500°C for 20 hrs had the largest grain as will be shown in Fig. 6, its largest grain boundary resistivity is very interesting.

In the applications, for the use of an electrolyte, the doped CeO_2 should have the resistivity as low as possible to decrease the polarization in that. The total resistivity of the sintered $(CeO_2)_{0.9}(Gd_2O_3)_{0.1}$ bodies measured at 800°C are shown in Fig. 3 as a rectangular bar with the sintering time. As the curves such as the arcs corresponding to the grain interior resistivity and grain boundary resistivity were not displayed in complex impedance plots at 800°C within the available frequency range of the HP 4192A apparatus. Then, the total resistivity at 800°C were obtained by the measurement using a four-point probe method for the rectangular bar specimens in place of the summation of the grain interior resistivity obtained on the impedance plots. As the sintering time increases the total resistivity decreases and then again increases at the sintering times more than 10 hrs. The minimum total resistivity at the sintering time of 10 hrs is lower as compared with the values reported by K. Egchi *et al.*[13] The total resistivity of the sintered $(CeO_2)_{0.9}(Gd_2O_3)_{0.1}$ bodies sintered at 1500°C for 10 hrs also had the minimum values from the complex impedance plots even at the other measuring temperatures in the ranges of 450~600°C. To examine the reasons for the lowest total resistivity of the $(CeO_2)_{0.9}(Gd_2O_3)_{0.1}$ bodies sintered at 10 hrs, Arrhenius plots of temperature-dependent electrical conductivities converted from the summations of grain interior resistivity and grain boundary resistivity for the sintered $(CeO_2)_{0.9}(Gd_2O_3)_{0.1}$ bodies are shown in Fig. 4. Over the temperature range examined (250~600°C) the slopes of the Arrhenius plots are linearly dependent on the measuring temperature. It can be, therefore, said the electrical conductivity of the sintered $(CeO_2)_{0.9}(Gd_2O_3)_{0.1}$ bodies is thermally activated with the equation (1);

$$\sigma=(\sigma_0/T)\exp(-E_a/RT) \quad (1)$$

Where E_a is the activation energy for ionic migration, σ is conductivity, T is temperature in K, and R is gas constant. This type of the Arrhenius plot was frequently reported in the crystalline extrinsic ionic conductors such as Y_2O_3-doped ZrO_2 and Gd_2O_3-doped ZrO_2.[14-15] It was well known that the doped CeO_2 was operated as a pure ionic conductor in air.[16-17] Here, the activation energy from the slope of the Arrhenius plot offers the information of electrical conduction mechanism in the materials.[17] Therefore, it can be thought that the sintered $(CeO_2)_{0.9}(Gd_2O_3)_{0.1}$ bodies have similar ionic conduction mechanisms regardless of the sintering times because of having almost the same slopes with the activation energies of 0.966~0.972 eV.

The activation energies from the temperature-dependencies of σT for the grain interior, grain boundary, total resistivities of the $(CeO_2)_{0.9}(Gd_2O_3)_{0.1}$ bodies sintered at 1500°C with the various sintering times are shown in Fig. 5. As the sintering time increases, the activation energy for the grain

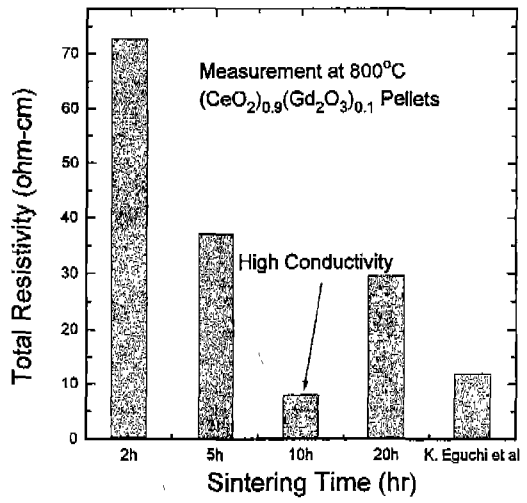

Fig. 3. The total resistivity of the sintered $(CeO_2)_{0.9}(Gd_2O_3)_{0.1}$ bodies with the sintering time.

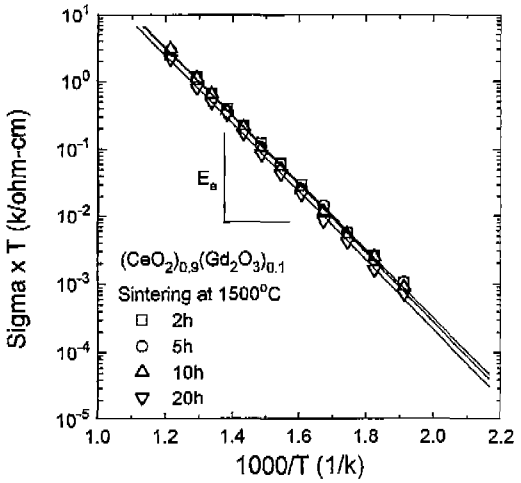

Fig. 4. Temperature-dependences of the electrical conductivities of the $(CeO_2)_{0.9}(Gd_2O_3)_{0.1}$ bodies sintered at 1500°C with various sintering times.

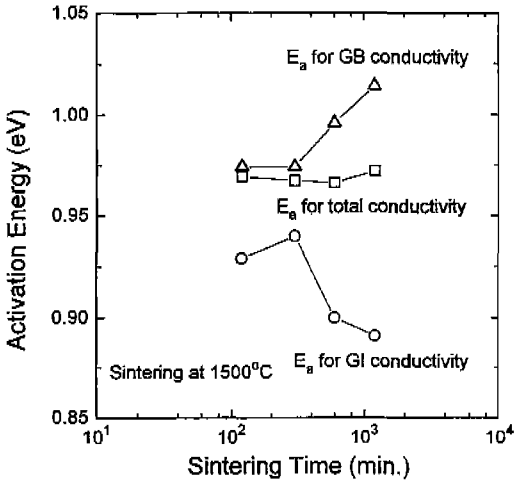

Fig. 5. The activation energies from the temperature-dependences for the grain interior, grain boundary, and total conductivities for the $(CeO_2)_{0.9}(Gd_2O_3)_{0.1}$ bodies sintered at 1500°C with the various sintering times.

interior resistivity decreases and reversibly that for the grain boundary resistivity increases. The activation energies from the total resistivity are induced from the combination between the activation energies for the resistivity had little change with the increase of the sintering time in Fig. 4, but shows the minimum values just at the sintering time of 10 hrs. Conclusively, the minimum total resistivity of the $(CeO_2)_{0.9}(Gd_2O_3)_{0.1}$ bodies sintered at 1500°C for 10 hrs appears to result from the lowest activation energy by their combinations between the activation energies for the resistivities at the grain interior and at grain boundary.

Fig. 6 shows the SEM photos of the $(CeO_2)_{0.9}(Gd_2O_3)_{0.1}$ bodies sintered at 1500°C for the various sintering times. It can be seen that the grain of the sintered $(CeO_2)_{0.9}(Gd_2O_3)_{0.1}$ bodies grows with the sintering time and there are no pores in the $(CeO_2)_{0.9}(Gd_2O_3)_{0.1}$ bodies for the sintering time more than 5 hrs.

On the other hand, the grain growth with the increase of the sintering time is expected to decrease the grain boundary resistivity and to increase the grain interior resistivity by the decrease of the grain boundary volume fraction. It was, however, confirmed that all the components of the resistivity in the sintered $(CeO_2)_{0.9}(Gd_2O_3)_{0.1}$ bodies had the minimum values at the sintering time of 10 hrs. It can be, therefore, thought from the variations of the electrical properties with the sintering time that the total resistivity of the sintered $(CeO_2)_{0.9}(Gd_2O_3)_{0.1}$ bodies, together with the grain growth, may decrease by the elimination of micro-pores or point defects and may increase by the segregation of Gd dopant, and/or the enhancement of the space charge regions at the grain boundary, considering from the occurrence of the largest grain boundary resistivity at the sintering time of 20 hrs as shown in Fig. 2. Then it may be thought that the microstructural changes such as the grain growth, the

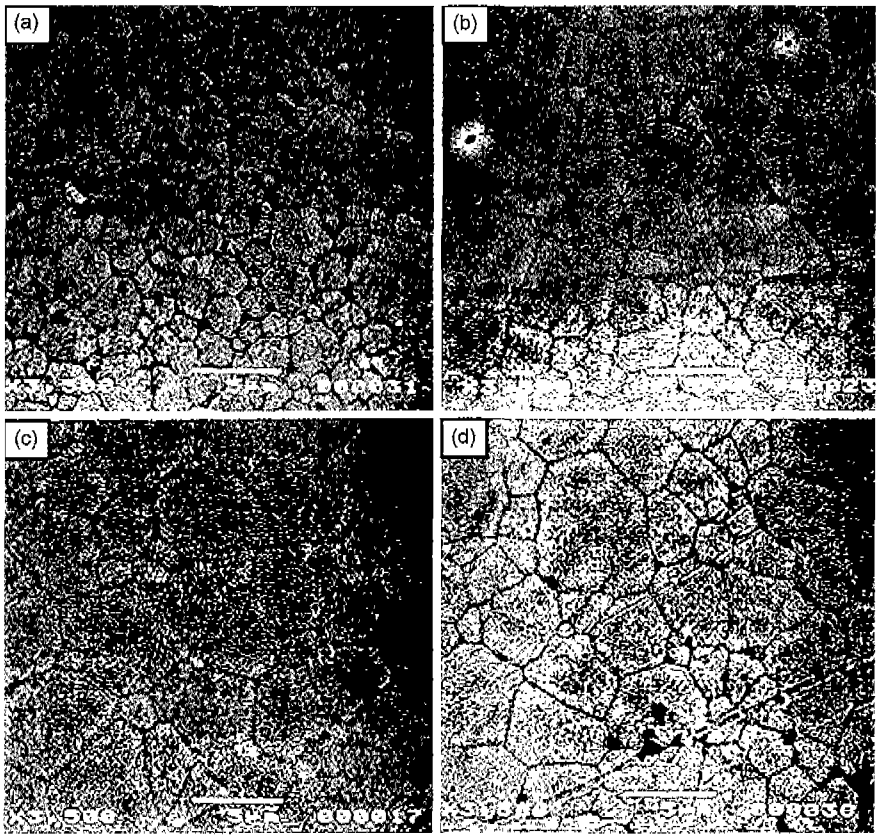

Fig. 6. SEM photos of the $(CeO_2)_{0.9}(Gd_2O_3)_{0.1}$ bodies sintered at 1500°C for (a) 2 hrs, b) 5 hrs, (c) 10 hrs and (d) 20 hrs in air, respectively.

segregation of the dopant, and/or the enhancement of the space charge regions at the grain boundary with the sintering time can induce the changes in the activation energies for the grain interior and grain boundary resistivity.[18-21] In the future, it will be required to investigate deeply the changes of the activation energies for the electrical conductivities of the sintered$(CeO_2)_{0.9}(Gd_2O_3)_{0.1}$ bodies for further understanding.

IV. Conclusions

The ultrafine $(CeO_2)_{0.9}(Gd_2O_3)_{0.1}$ solid solution powders, synthesized by the GNP, with specific surface areas of 19~23 m^2/g were sintered at 1500°C for the various sintering times in air and then their electrical characteristics were investigated with AC impedance and four-probe methods in air. The electrical resistivity of the sintered $(CeO_2)_{0.9}(Gd_2O_3)_{0.1}$ bodies decreased with the increase of the sintering time and then showed the minimum value at the sintering time of 10 hrs. The minimum total resistivity of the $(CeO_2)_{0.9}(Gd_2O_3)_{0.1}$ bodies sintered at 1500°C for 10 hrs seems to result from the lowest activation energy for the electrical conduction by the combination between the activation energies at the grain interior and grain boundary. And the lowest activation energy for this resistivity may result from the microstructural changes such as the grain growth, the segregation of the dopant, and/or with the enhancement of the space change regions at the grain boundary with the sintering time.

References

1. B. C. H. Steele, "Oxygen Transport and Exchange in Oxide Ceramics," *Journal of Power Sources JPS Switzerland,* **49**(1-3), 1-14 (1994).
2. B. G. Pound, "Response to Comment by J. Ranlov, F. W. Poulsen and M. Mogensen on The Characterization of doped CeO_2 Electrodes in Solid Oxide Fuel Cells," *Solid State Ionics,* **61**, 281-84 (1993).
3. M. Sahibzada, B. C. H. Steele, K. Zheng, R. A. Rudkin and I. S. Metcalfe, "Evelopment of Solid Oxide Fuel Cells Based on a $Ce(Gd)O_{2-x}$ Electrolyte Film for Intermediate Temperature Operation," *Catalysis Today,* **38**(4), 459-66 (1997).
4. J. Ranlov, E. W. Poulsen and M. Mogensen, "Comment on The Characterization of Doped CeO_2 Electrodes in Solid Oxide Fuel Cells by B. G. Pound, Solid State Ionics 52 (1992) 183-188," *Solid State Ionics,* **61**, 277-79 (1993).
5. A. D. S. Costa, J. A. Labrincha and F. M. B. Marques, "p-type Conductivity in Gadolinia-doped Ceria," *Journal of Materials Science Letters,* **15**(19), 1716-18 (1996).
6. M. Hirano and E. Kato, "Hydrothermal Synthesis of Cerium(IV) Oxide," *J. Am. Ceram. Soc.,* **79**(3), 777-80 (1996).
7. Y. Konishi, T. Murai and S. Asai, "Preparation and Characterization of Fine Ceria Powders by Hydrolysis of Cerium(III) Carboxylate Dissolved in Organic Solvent," *Industrial & Engineering Chemistry Research,* **36**(7), 2641-45 (1997).
8. M. N. Rahaman, *Ceramic Processing and Sintering.* Marcel Dekker Inc., New York, 1995.
9. N. J. Hess, G. D. Mauldin, L. A. Chick, D. S. Sunberg, D. E. McCreedy an T. R. Armstrong, "Synthesis and Crystallization of Yttrium-aluminium Garnet and Related Compounds," *J. Mater. Sci.*, **29**(7), 1873-78 (1994).
10. L. A. Chick, L. R. Pederson, G. D. Maupin, J. L. Bates, L. E. Thomas and G. J. Exarhos, "Glycine-nitrate Combustion Synthesis of Oxide Ceramic Powders," *Mater. Lett.,* **10**, 6-12 (1990).
11. S. R. Jain, K. C. Adiga and V. R. Pai Verneker, "A New Approach to Thermochemical Calculations of Condensed Fuel-Oxidizer Mixtures," *Combustion & Flame,* **40**, 71-79 (1981).
12. D. Y. Wang and A. S. Nowick, "Diffusion-controlled Polarization of Pt, Ag, Au Electrodes with Doped Ceria Electrolyte," *J. Electrochem. Soc.,* **128**, 55-63 (1981).
13. K . Eguchi, T. Inoue, M. Udea, J. Kamimae and H. Arai, "The Activation and Transfer of Oxygen at Electrolyte/Cathode Interface for SOFCs," pp. 697-704 in *Proceedings of the 2nd International Symposium on SOFCs*, Edited by F. Gross, P. Zegers, S. C. Singhal and O. Yamamoto. Commission of The European Communities, Luxembourg, 1991.
14. A. Ovenston, "A Effect of Atmosphere on the Electrical Properties of Polycrystalline Yttria-stabilised Zirconia," *Solid State Ionics* **58**(3-4), 221-29 (1992).
15. T. K. Kang, T. Nagasaki, N. Igawa, K. Il-Hiun and H. Ohno, "Electrical Properties of Cubic, Stabilized, Single ZrO_2-Gd_2O_3 Crystals," *J. Am. Ceram. Soc.,* **75**(8), 2297-99 (1992).
16. R. N. Blumenthal, F. S. Brugner and J. E. Garnier, "The Electrical Conductivity of CaO-doped Nonstoichiometric Cerium Oxide from 700°C to 1500°C," *J. Electrochem. Soc.,* **120**, 1230-37 (1973).
17. H. L. Tuller and A. S. Nowick, "Doped Ceria as a Solid Oxide Electrolyte," *J. Electrochem. Soc.,* **122**, 255-59 (1975).
18. N. Bonanos, *Impedance Spectroscopy.* John Wiley & Sons, New York, 1987.
19. B. C. H. Steele, P. H. Middleton and R. A. Rudkin, "Material Science Aspects of SOFC Technology with Special Reference to Anode Development," *Solid State Ionics* **40/41**, 388-93 (1990).
20. L. M. Levinson, "Grain Boundary Phenomena in Electronic Ceramics," pp.120-146 in *Advances in Ceramics.* Edited by D. C. Hill. Am. Ceram. Soc., Columbus, Ohio, 1981.
21. L. Heyne, "Interfacial Effects in Mass Transport in Ionic Solids," pp. 425-456 in *Mass Transport in Solids.* Edited by F. Beniere, and C. R. A. Catlow. Plenum Press, New York, 1983.